

# X-ray Tube Monte Carlo Model Based on GEANT4 to Optimize Excitation Energy Spectrum and Source Collimator Design for X-ray Fluorescence Imaging

R. SCHMIDT<sup>1</sup>, J. SHI<sup>1</sup>, J. FORD<sup>1</sup>

<sup>1</sup> University of Miami, Departments of Radiation Oncology and Biomedical Engineering

## INTRODUCTION

X-ray fluorescence computed tomography (XFCT) as a new modality has gained wide interest in the field of molecular imaging in recent years [1]. By collecting the characteristic x-ray fluorescence (XRF) photons, whose intensity corresponding to the element's concentration, the probes within the sample can be localized and quantified. Because the photoelectric absorption probability is proportional to  $Z^3$  [2], high- $z$  materials are the best suitable probes for XFCT imaging. Gold nanoparticles (GNPs) have shown a dose enhancement ratio [3], low attenuation of the K-shell fluorescence photons, and can preferentially accumulate in tumors via enhanced permeability and retention [4] – these factors make GNPs ideal for XFCT imaging of malignancies. In order to create the photoelectric effect, however, the incident photons need to have kinetic energy greater than the binding energy of the K-shell electrons. The binding energy for Gold K-shell electrons is 80.7 keV, while the K-shell emission of Gold is 67.0 keV and 68.8 keV for  $K_\alpha$  and  $K_\beta$  respectively. Above the K-edge, the photoelectric interaction probability begins to fall off as  $1/E^3$  [2].

## AIM

To optimize the excitation energy spectrum for GNP K-shell XFCT imaging, we developed a computational model (based on Geant4) of a benchtop x-ray tube. By simulating the design of excitation filter and source collimator the system can be optimized while saving time, cost, and labor.

## METHOD

1. The Monte Carlo model was developed using the Geant4 toolkit (release 10.6). The dual-focal-spot x-ray tube (Model MXR 225/22, COMET) [5] was employed as the excitation source for XFCT imaging (see Fig. 1).
2. The computational x-ray source was filled with vacuum, and included a virtual monoenergetic electron gun (to simulate 2-cm W filament), a rectangle W-target cut at 20 degree angle, and a 0.8-mm Be window (inherent filter).
3. The electron beam strikes the W-target with a spot size of 5.5 mm to mimic the operation conditions of the benchtop x-ray tube for XFCT imaging.
4. The physics list was derived from PENELOPE [6], where the photoelectric effect, Compton Scattering, Rayleigh scattering, Coulomb scattering, ionization, multiple scattering, and bremsstrahlung were included.
5. Small adjustments were made to the collimation and filtration thickness and material type until the produced energy spectrum was best suited for K-shell XRF. Several of the energy spectrums are shown in the results sections (see Fig 2-4).
6. The collimator was designed using Cerrobend and a visual test was done in order to ensure there was no leakage.

## RESULTS

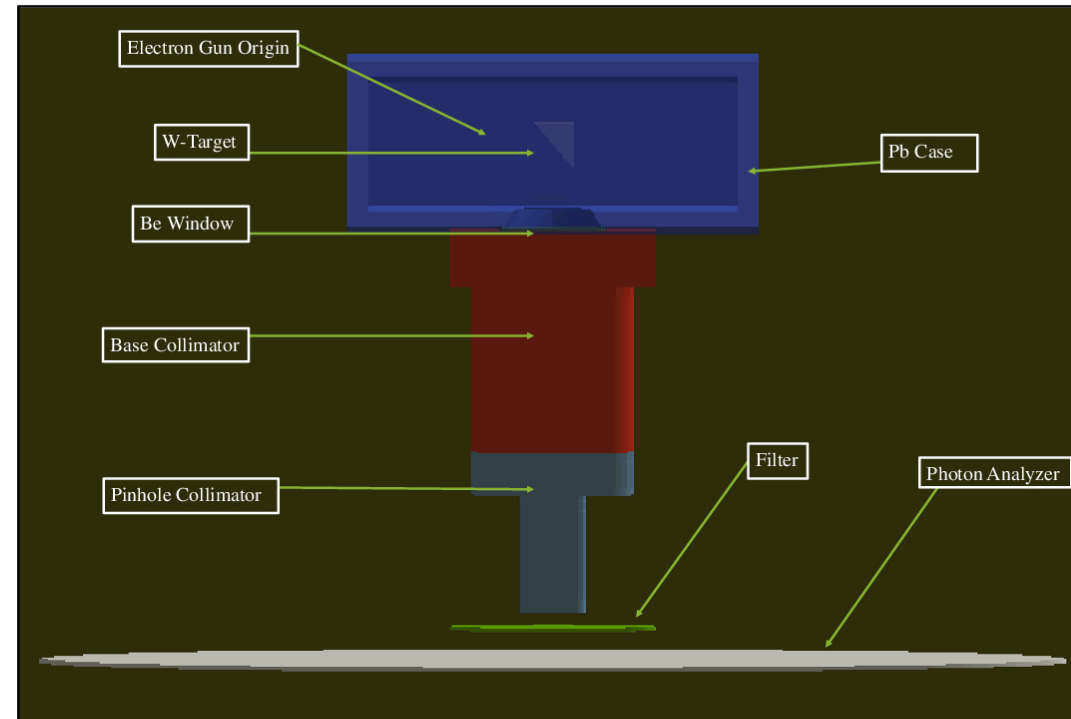


Fig. 1. The geometry of the simulated x-ray tube with collimation and filtration. The tube consists of the electron gun, the W-target cut at 20 degrees to the incoming beam, a window cutout of the Pb casing, and the inherent 0.8 mm Be window. The base collimator (red part) shapes the beam into a 5 mm pencil beam. The pinhole collimator (blue part) further shapes the beam into a 0.71 mm pencil beam. A filter can be seen at the exit of the collimation and finally the photon analyzer is shown in gray near the bottom.

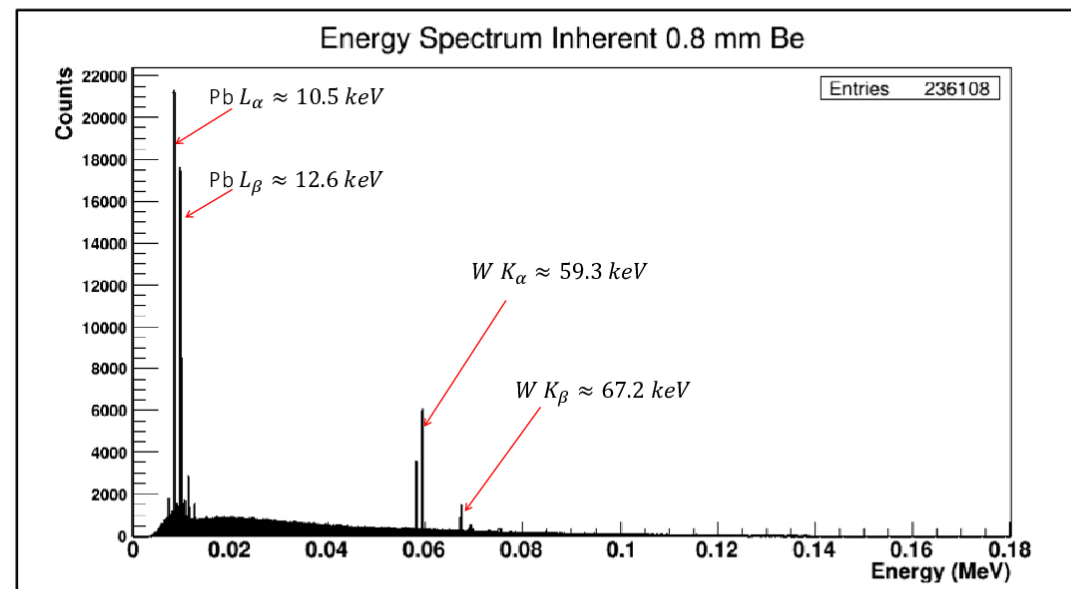


Fig. 2. Energy spectrum of the unfiltered x-ray output with an electron gun energy of 150 keV and no collimation. Characteristic energy peaks originating from the Pb casing and W-target are marked by the red arrows. The number of entries corresponds to the number of photons recorded by the photon analyzer with 100 million initial electrons. This spectrum was used in order to confirm the physics toolkit was implemented correctly.

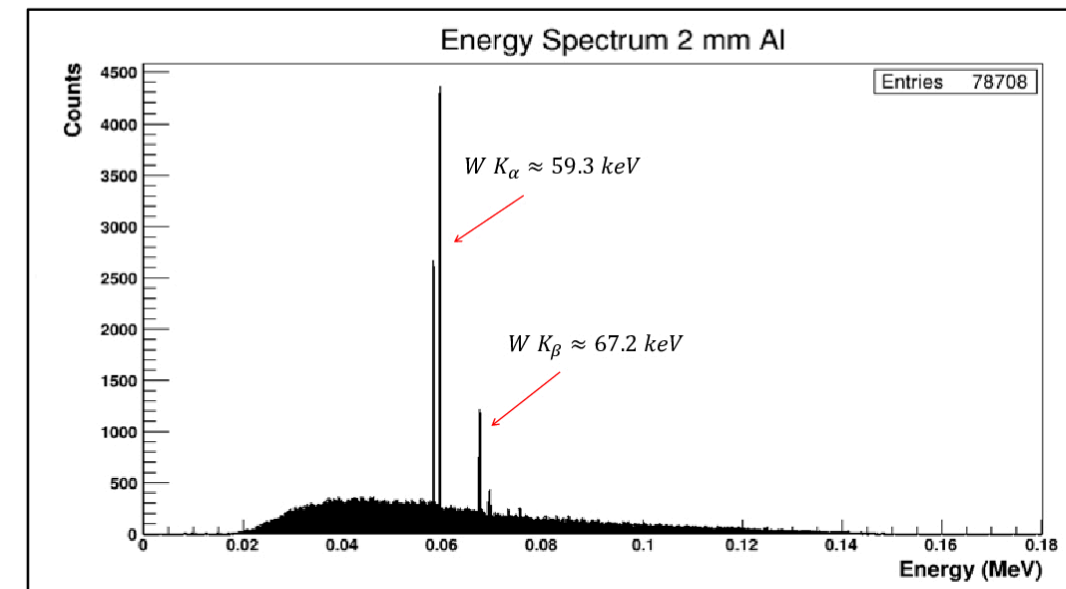


Fig. 3. X-ray output with a gun energy of 150 keV and no collimation after passing through a 2.0 mm Al filter. The characteristic energy peaks of the Tungsten-target at 59.3 keV and 67.2 keV are marked by the red arrows. The number of entries corresponds to the number of photons recorded passing through the photon analyzer with 100 million initial electrons. Many filter iteration were made, with different filter materials and thicknesses, including this 2 mm Al filter. The result of the 2.0 mm Al filter has an energy spectrum with lower median and mean energies than the binding energy of Gold K-shell electrons.

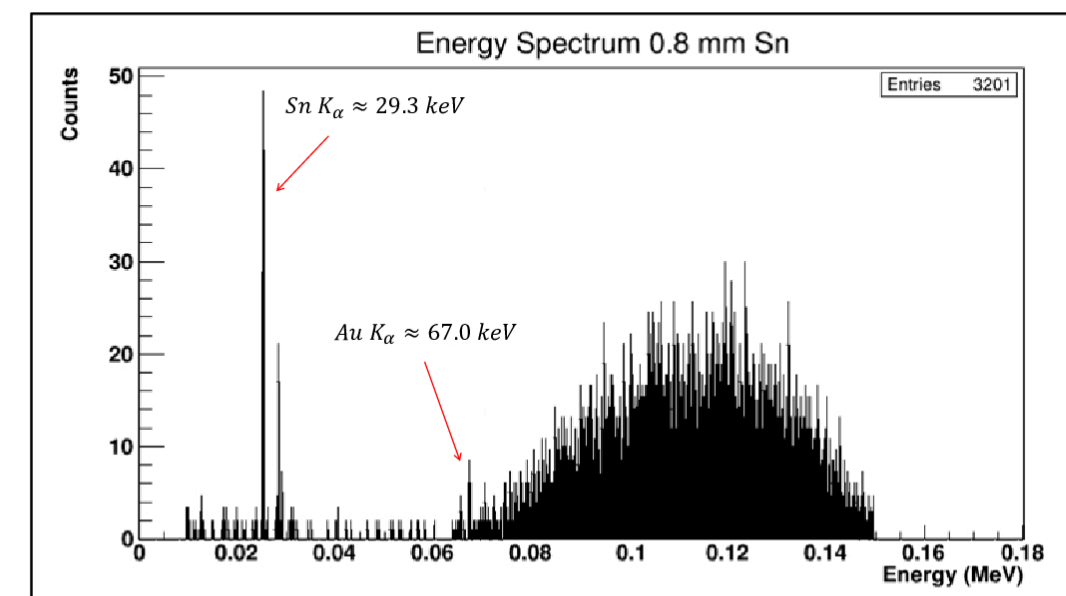


Fig. 4. X-ray output with a gun energy of 150 keV and no collimation after passing through a 0.8 mm Sn filter. Notice the characteristic energy peaks of the Sn at 29.3 keV marked by the red arrow. The Gold K-edge is shown on this figure in order to show where the energy output should be minimized to avoid interference. The number of entries corresponds to the number of photons passing through the photon analyzer with 100 million electrons used.

## CONCLUSIONS

For GNP XFCT, the optimal energy spectrum has minimal to no background at energies both above and below the binding energy of the K-shell electrons. Gold K-shell electrons have a binding energy of 80.7 keV, thus having a signal with a peak at or just above 80.7 keV will result in more fluorescence photons. These fluorescence photons will be emitted with an energy of 67.0 keV and 68.8 keV for  $K_\alpha$  and  $K_\beta$  respectively, motivating the filter to minimize the background in this region. Through the iterative process of testing many different filter materials and thicknesses the optimal filtration for Gold nanoparticle K-edge x-ray fluorescence was determined to be 0.8 mm of Sn. Several different collimation materials were tested in order to ensure leakage was at a minimum. Using a visual test a suitable pinhole Cerrobend collimator was designed. Our Geant4 simulation is capable of simulating physics interactions, geometries and produce acceptable data for the future XFCT imaging studies. Monte Carlo computational models can expedite the process of XRF system development and optimization, which saves costs, time and labor.

## ACKNOWLEDGEMENTS

I would like to thank Dr. Ford and Dr. Shi for their support and guidance on this project. I would also like to specifically thank Dr. Shi for his help implementing the Geant4 script.

## REFERENCES

- [1] Haschke, Michael. "XRF-Basics." *Laboratory Micro-X-Ray Fluorescence Spectroscopy Springer Series in Surface Sciences*, 2014, pp. 1–17., doi:10.1007/978-3-319-04864-2\_1.
- [2] "X-Ray Interactions." *Review of Radiologic Physics*, by Walter Huda, Lippincott Williams And Wilkin, 2016, pp. 17–20.
- [3] Sharma, Sunildutt, and Nitinramesh Kakade. "Dose Enhancement in Gold Nanoparticle-Aided Radiotherapy for the Therapeutic Photon Beams Using Monte Carlo Technique." *Journal of Cancer Research and Therapeutics*, vol. 11, no. 1, 2015, p. 94., doi:10.4103/0973-1482.147691.
- [4] Kalyane, Dnyaneshwar, et al. "Employment of Enhanced Permeability and Retention Effect (EPR): Nanoparticle-Based Precision Tools for Targeting of Therapeutic and Diagnostic Agent in Cancer." *Materials Science and Engineering: C*, vol. 98, 2019, pp. 1252–1276., doi:10.1016/j.msec.2019.01.066.
- [5] "COMET X-Ray - MXR-225/22." *Ray*, www.comet-xray.com/en/products/x-ray/tubes/tubes/mxr-225-22.
- [6] Baró, J., et al. "PENELOPE: An Algorithm for Monte Carlo Simulation of the Penetration and Energy Loss of Electrons and Positrons in Matter." *Nuclear Instruments and Methods in Physics Research Section B: Beam Interactions with Materials and Atoms*, vol. 100, no. 1, 1995, pp. 31–46., doi:10.1016/0168-583x(95)00349-5.

## CONTACT INFORMATION

E-mail: rms319@miami.edu